

3VL: Using Trees to Improve Vision-Language Models' Interpretability

Nir Yellinek, Leonid Karlinsky and Raja Giryes, *Senior IEEE*

Abstract—Vision-Language models (VLMs) have proved effective at aligning image and text representations, producing superior zero-shot results when transferred to many downstream tasks. However, these representations suffer some key shortcomings in Compositional Language Concepts (CLC) understanding such as recognizing objects' attributes, states, and relations between different objects. Moreover, VLMs typically have poor interpretability, making it challenging to debug and mitigate compositional-understanding failures. In this work, we introduce the Tree-augmented Vision-Language (3VL) model architecture and training technique accompanied by our proposed Anchor inference method and Differential Relevance (DiRe) interpretability tool. By expanding the text of an arbitrary image-text pair into a hierarchical tree structure using language analysis tools, 3VL allows inducing this structure into the visual representation learned by the model, enhancing its interpretability and compositional reasoning. Additionally, we show how Anchor, a simple technique for text unification, can be employed to filter nuisance factors while increasing CLC understanding performance, e.g., on the fundamental VL-Checklist benchmark. We also exhibit how DiRe, which performs a differential comparison between VLM relevancy maps, enables us to generate compelling visualizations of the reasons for a model's success or failure.

I. INTRODUCTION

In recent years, Vision-Language models (VLMs) have emerged as a powerful tool for tasks such as image captioning, visual question answering, and image retrieval. These models have achieved remarkable success owing to their ability to align visual and textual features and extract meaningful information from them. However, these models have several limitations in understanding Compositional Language Concepts (CLC) such as recognizing objects' attributes, states, and relations between different objects. While VLMs have shown remarkable performance in zero-shot transfer learning, their results are not interpretable and they typically struggle with compositional reasoning, where they need to understand the relationships between different concepts in a sentence to provide an accurate response.

Previous works on improving compositionality in VLMs focused mostly on augmenting data points in text space [1]–[5]. While this approach has led to some performance improvements, it offers no extra interpretability. Several approaches have been proposed for interpreting neural networks ranging from attribution methods to visualization techniques [6]–[12]. However, most are designed to explain an already trained network, and interpretability is often limited to a local and task-specific context [13]–[20]. Thus, it has been suggested that a better approach is explainability by design [21], i.e., interpretability is built into the model architecture and training process. By doing so, a more general and systematic

interpretation and analysis of the model is enabled. This makes it easier to identify failure modes and biases early in the development process. Furthermore, such an approach provides visualizations that can help users understand and analyze the model's behavior, making it more transparent and trustworthy. In this paper, we take a step towards facilitating such explainability for VLMs.

We propose a novel approach to address VLMs' limitations in compositional understanding and interpretability by leveraging natural language hierarchical structures. Our approach is based on the idea of expanding the text of an image-text pair into a hierarchical tree structure using language analysis tools, and inducing this structure into the visual representation learned by the model. Specifically, we propose the Tree-augmented Vision-Language (3VL) model architecture and training technique, which allows for rich exploration of the text space using several levels of incremental text augmentation from coarse to fine-grained. Each level of the tree represents a progressive refinement of the text structure and captures an increasingly detailed aspect of the image-text relationship. We use this hierarchical structure to guide the learning of visual features in a way that improves the model's compositional reasoning ability.

To complement our tree-based structured method, we introduce two novel inference and interpretability techniques called Anchor and Differential Relevance (DiRe). These approaches extract image relevancy maps using HilaCAM [22] based on positive and negative texts. By comparing the relevancy maps of images with positive text to that of the same image with negative text, these strategies can identify further weaknesses of VLMs and filter out the noise and irrelevant information from the input. This leads to an increase in VLMs' performance on Compositional Language Concepts tasks. Furthermore, our proposed techniques also provide insights into the underlying failure modes of the used models.

We evaluate our approach on popular Compositional Language Concepts benchmarks and demonstrate that our method achieves state-of-the-art performance, outperforming existing VLM-based methods on these tasks. Furthermore, we show that our approach is not only effective but also interpretable, enabling us to both generate compelling visualizations of the reasons for model success or failure and effectively filter the image signal for increased performance.

This paper is organized as follows. In Section I we briefly describe the topics related to this research and the main goals of this work. In Section II, we provide the necessary background and review the existing literature on related topics. In Section III, we present our novel tree-based training technique and inference method. This approach improves the

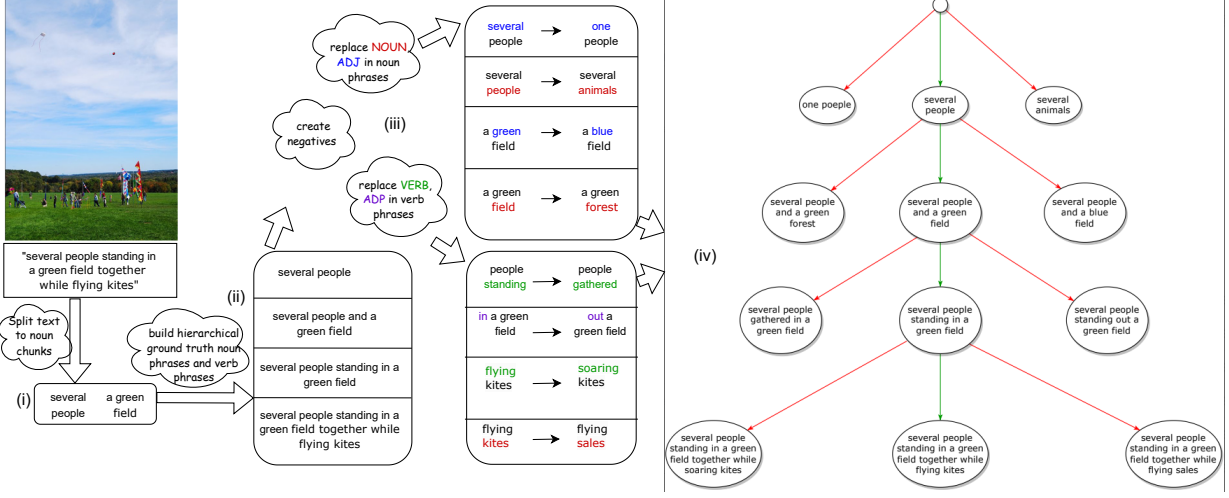


Fig. 1. The caption tree generation flow: (i) parse the sentence to get noun phrases and part of speech (ii) hierarchically reconstruct the caption (iii) generate negatives for each sub-caption (iv) compose the final tree.

interpretability of VLMs. In Section IV, we provide additional interpretability tools. In Section V, we conduct experiments to test the effectiveness of our proposed methods. Finally, in Section VI, we summarize our contributions and propose some ideas for possible future work.

II. BACKGROUND

This section begins with a review of existing methods for interpretability of deep neural networks and then discusses the usage of trees for deep learning and how our approach differs from previous works. Finally, it describes existing efforts for compositional understanding in VLMs.

A. Interpretability of deep neural networks

Many approaches have been developed for explaining the decisions of neural networks [21], [23]. Most works interpret decisions of an already trained network. Gradient Saliency [6], GradCAM [7] and Integrated Gradients [9] use convolutional neural network gradients to find significant pixels in the input that impact the network output. LIME [8] and SHAP [10] segment first the input into super-pixels in order to find regions that explain the output. Wavelets [11] and Shearlets [12] have been used in order to further improve the region selection. In order to provide similar interpretability tools for transformers, Chefer et al. [24] proposed to use the concept of layer-wise Relevance Propagation [25], with gradient integration for the self-attention layers of transformers. HilaCAM [22] proposed a more general approach that can visualize transformer architectures more easily.

Another line of work focuses on ‘explainability by design’ pointing to some flaws [13], [14], [16]–[20], [26] in existing solutions for neural networks that are already trained. Instead, it is suggested to incorporate interpretable features in the model’s structure. One approach generates a set of linear transformations that are applied to the input [27]. Another strategy encourages the network to make decisions that are locally linear [28]. This linearity makes the decision more interpretable. Another method [29] generates a sequence of queries and makes a decision based on them. In [30] a

variational model is used to optimize the queries usage. An alternative approach is to learn interpretable semantic concepts from the data and then make a decision based on them [31]–[35]. A similar technique teaches the network to output also a ‘why’ concept in addition to its decision [36]. Another work has incorporated a star model into network learning to get a relationship between locations in the query image and the decision of the network [37].

B. Tree usage for deep learning

Trees have been used with neural networks in different constellations [38]. They have been incorporated into LSTMs [39] for improving semantic representations. Tree LSTMs have been combined with dependency parsing trees (DPTs) to improve visual grounding [40]. In [41], [42] decision trees were combined with the representation learning functionality of neural networks. In [43] tree were used with VLMs for improving their grammar induction in an unsupervised manner.

For improving the explainability of the network, a random forest has been trained on the network data and its decisions were used to regularize the neural network such that it generates axis aligned decisions [44]. Random forests have also been used in conjunction with pre-trained neural networks for improving the robustness of the latter to adversarial attacks [45], [46]. Another strategy that uses trees to improve interpretability is NBDT [47] that replaces the neural network final layer with a decision tree, which helps to understand better the neural network mistakes.

C. Compositional understanding in Vision-Language Models

One of the key challenges in developing effective vision and language models (VLMs) is achieving a compositional understanding of the underlying visual and linguistic elements.

Some VLMs such as CLIP [48] and ALIGN [49] have shown great progress in zero-shot downstream tasks by pre-training on a large-scale dataset of text-image pairs collected from the web using contrastive image-text alignment. Other approaches like LXMERT [50], UNITER [51], and

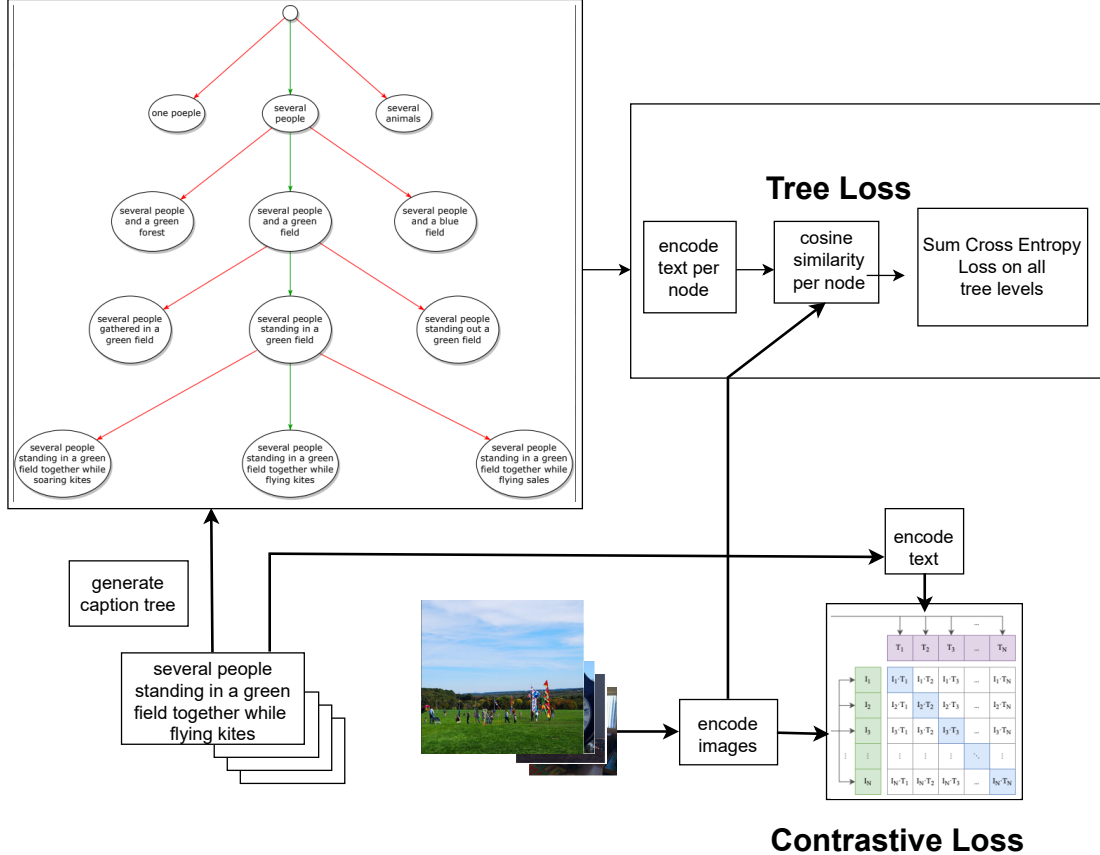


Fig. 2. The tree loss and contrastive loss that are used for training 3VL. For the tree loss we first generate a caption tree and then sum the cross entropy loss in all tree levels. For the contrastive loss we calculate the average cross entropy loss over all image-text pairs in the batch.

OSCAR [52] utilize off-the-shelf object detectors to extract region features.

More recent works have explored techniques for fine-grained contrastive learning and additional positives from nearest neighbors to improve image-text retrieval on benchmarks such as ImageNet [53] and MS-COCO [54]. These models include FILIP [55], CyClip [56], DeCLIP [57], and PyramidCLIP [58].

Some recent works propose self-supervised learning objectives such as image-text matching and masked/autoregressive language modeling to improve the model's ability to understand vision and language concepts. These works include VILT [59], ALIGN [49], Vision-TALK [60], ViCHA [61] and BLIP [62]. BLIP, for example, generates synthetic captions from the language modeling head and filters noisy captions based on the image-text matching score.

Despite these advances, recent studies like VL-CheckList [63], the Winoground Challenge [64], VSR [65] and COLA [66] have shown that VLMs still struggle with understanding fine-grained language details and Compositional Language Concepts (CLC). Another work has shown that there is a fundamental challenge for transformers with compositionality [67]. Therefore, there is still much work to be done in developing VLMs with stronger compositionality and robustness to complex, real-world scenarios.

Achieving a full understanding of the semantics of rich visual scenes involves the ability to detect individual entities, reason about their interactions and attributes, and ultimately

understand the visual concepts within the scene. Structured representations have played a vital role in this process, and have been applied to a wide range of computer vision applications, such as vision and language [52], [68]–[70], scene graphs [71]–[75], relational reasoning [76], [77], human-object interactions [78]–[80], action recognition [81]–[87], and even image and video generation from graphs [88]–[90]. However, most of these works rely on detailed, manually curated supervision that often involves the annotation of location information and structural details. This results in limited-size or synthetic data sources for training, which can limit the effectiveness of the model. In [1], the authors have proposed a method for teaching CLC to large VLMs using only the available large-scale noisy Vision-Language data sources collected from the web, without the use of expensive manual curation. This approach aims to improve the scalability and effectiveness of VLMs' understanding of Compositional Language Concepts.

Perhaps most similar to our augmentation method is the work of [1], which generates one negative caption per example by replacing one random word out of all possible candidates. Our proposed approach differs from the above by generating several augmentations per caption in the form of hierarchical trees for VLM training. Note that unlike previous works on compositionality in VLMs, our approach aims at improving both compositional reasoning and interpretability.

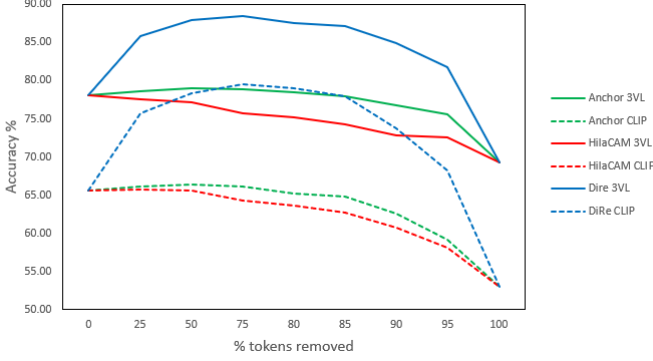


Fig. 3. 3VL Token Removal accuracy on VL-Checklist (average of Attribute and Relation). HilaCAM vs. Anchor vs. *DiRe* for both 3VL and vanilla CLIP. Notice that 3VL gets better accuracy compared to vanilla CLIP and its relative improvement with Anchor is better. Note that better improvement by *Token Removal* indicates that a better understanding of the token importance is gained and therefore there is a better interpretability.

III. THE TREE-AUGMENTED VISION-LANGUAGE (3VL) MODEL

This section describes 3VL, our novel tree-based model architecture and training technique, and our novel *Anchor* inference method and **Differential Relevance** (*DiRe*) interpretability tool. First, we present our tree augmentation technique. Then, we discuss the details of our tree-based training method. In Section IV, we present our *Token Removal* inference and interpretability tools.

A. Caption tree generation

We present below our tree augmentation method. Figure 1 illustrates this process.

- 1) For each image caption pair we first parse the caption using [91] to get all noun phrases and part of speech tags.
- 2) Then, we reconstruct the full caption hierarchically from coarse to fine-grained to get a positive sub-caption for each level in the tree in the following way:
(using the caption “several people standing in a green field together while flying kites” as an example)
 - 2.1 The first level of the tree will contain the first noun phrase as its positive text (i.e. “several people”).
 - 2.2 The second level of the tree will contain the text of the first and second noun phrases concatenated with some connecting word like ‘and’ (i.e. “several people and a green field”).
 - 2.3 The third level of the tree will contain the text of the original caption from the start until the end of the second noun phrase (i.e. “several people standing in a green field”).
 - 2.3.1 If more noun phrases exist in the original caption then in a similar way the next levels of the tree will contain the text of previous noun phrases concatenated to the current noun phrase with a word like ‘and’, and the original caption from the start until the end of the current noun phrase.
 - 2.4 Finally, the last level of the tree will contain the text of the full original caption (i.e. “several people standing in a green field together while flying kites”).

3) Next, in each tree level we generate one negative caption for each Noun, Adjective, Adposition, and Verb of the positive text (each negative replaces just one word in the original caption). Note that we do not replace again words that appeared in previous tree levels. So information from a previous level flows without change. Each negative word is generated as follows:

- 3.1 Find an opposite (Antonym) of the positive word using FLAN-T5 LLM [92] with prompt (e.g. “find an opposite for the word: <>”).
- 3.2 If an opposite is not found, we generate a co-hyponym¹ of the positive word using NLTK’s [93] WordNet [94] module.
- 3.3 If a co-hyponym is not found, we use T5 LLM [95] to generate a word to fill in a masked positive word (the token ‘<extra_id_0>’ replaces the positive word in the prompt).

For the above example caption we generate the following negative captions:

- At the first level we generate, for the positive text “several people”, the negative texts “one people” and “several animals”.
- At the second level we generate, for the positive text “several people and a green field”, the negative texts “several people and a blue field” and “several people and a green forest”.
- At the third level we generate, for the positive text “several people standing in a green field”, the negative texts “several people gathered in a green field” and “several people standing out a green field”.
- At the fourth level we generate, for the positive text “several people standing in a green field together while flying kites”, the negative texts “several people standing in a green field together while soaring kites” and “several people standing in a green field together while flying sales”.

Note that our automated negatives generation method can generate grammatical errors sometimes.

B. Tree-based training

CLIP contrastive loss. Given a batch of N image-caption pairs we extract the image and text representations, I_r and T_r , using CLIP’s image and text encoders. Then, we compute the pairwise cosine similarity scores $S_{j,k}$ for each image j and caption k in the batch. From the similarities matrix we calculate the cross entropy loss with softmax over the rows (\mathcal{L}_{img}) and the cross entropy loss with softmax over the columns (\mathcal{L}_{txt}). The final CLIP contrastive loss is the average of these two losses:

$$\mathcal{L}_{contrast} = \frac{\mathcal{L}_{img} + \mathcal{L}_{txt}}{2}. \quad (1)$$

Tree-based loss. For each image-caption pair, we first create a caption tree. Then, for each level of the tree we calculate the cosine similarity scores between the image and all captions at

¹Co-hyponyms are words that share the same hypernym in the wordnet tree (e.g. “apple” and “banana” are co-hyponyms as they share the hypernym “fruit”; the words “car” and “motorcycle”, “blue” and “yellow” are co-hyponyms as well).

TABLE I

TOP-1 ACCURACY ON VL-CHECKLIST VG RELATION AND ATTRIBUTE DATASETS, WITH OPENAI CLIP VIT-B/32, NEGCLIP [98], RB+LLM NEGS [1], AND 3VL. TR STANDS FOR *Token Removal* (WE REMOVE FROM LOW TO HIGH IMPORTANCE). TOKEN IMPORTANCE IS TAKEN FROM RELEVANCY MAPS GENERATED BY [22] ON THE IMAGE WITH DIFFERENT TEXTS. ANC = ANCHOR (OURS) - TAKES THE PART OF TEXTS THAT DIFFER FROM EACH OTHER.

Model	Att Color	Att Material	Att Size	Att Action	Att State	Rel Action	Rel Spatial	Avg
CLIP [48]	66.68	67.25	67.90	73.31	71.09	60.80	55.90	66.13
NegCLIP [98]	73.62	75.83	66.12	75.37	70.24	66.18	60.87	69.75
RB+LLM Negs [1]	82.70	84.90	78.10	71.60	75.13	70.00	78.40	77.26
Our 3VL	75.29	82.63	70.90	81.10	75.03	81.69	81.14	78.25
Our 3VL + 65% TR ANC	76.18	82.51	71.36	79.57	76.63	83.73	84.29	79.18

TABLE II

TOP-1 ACCURACY ON VL-CHECKLIST VG OBJECT DATASET, WITH OPENAI CLIP VIT-B/32, NEGCLIP [98], RB+LLM NEGS [1], AND 3VL. AS AN ABLATION WE ALSO COMPARE TO CLIP AND CLIP+LORA THAT WERE TRAINED WITHOUT TREE-BASED LOSS.

Model	Location Center	Location Margin	Location Mid	Size Large	Size Medium	Size Small	Avg
CLIP	86.95	77.75	72.75	85.50	80.50	70.60	79.01
CLIP contrastive	88.53	73.42	81.44	89.71	80.03	73.98	81.18
CLIP+LoRA contrastive	88.04	72.29	80.77	89.62	79.35	71.68	80.29
NegCLIP	89.61	72.64	81.88	90.33	80.82	73.95	81.54
RB+LLM Negs	91.70	83.20	78.90	90.30	84.55	77.00	84.34
Our 3VL	93.82	85.02	89.48	94.96	88.61	83.78	89.28

that level and calculate the Cross Entropy Loss. The final tree loss, \mathcal{L}_{tree} , is the sum of losses over all tree levels (Fig. 2).

To preserve as much of CLIP’s zero-shot capabilities we also include $\mathcal{L}_{contrast}$, on the original MS-COCO dataset [54] (without extra negatives). Our final loss function is:

$$\mathcal{L}_{total} = \alpha \cdot \mathcal{L}_{tree} + (1 - \alpha) \cdot \mathcal{L}_{contrast}, \quad (2)$$

where $0 < \alpha < 1$ is a hyperparameter. We found $\alpha = 0.5$ to work the best.

To further diminish zero-shot forgetting, we also employ LoRA [96], following the work of [1] and train only the LoRA adapters while the base CLIP model parameters remain frozen.

Training Details. We finetune OpenAI CLIP [48] ViT-B/32 [97] with rank=1 LoRA adapters on the training set of MS-COCO [54] for 12 epochs. We use AdamW optimizer with learning rate $3e - 6$ and weight decay 0.1 and train with a batch size of 64 on a single GeForce RTX 2080 Ti NVIDIA GPU. We performed a hyperparameter sweep and chose final parameters and number of epochs based on MS-COCO validation set.

IV. RELEVANCY MAPS BASED TOKEN REMOVAL AND INTERPRETABILITY

A. Token Removal

Token Removal removes the least significant image tokens according to a given relevancy map. Then, the image with the removed tokens is used as input to the image encoder. We call this approach HilaCAM with *Token Removal*.

Using the relevancy maps generated for each image-text pair and *Token Removal* we point the model towards the more important parts of the image. By taking into account the relevancy maps of an image paired with a positive text and the same image paired with a negative text simultaneously, we are able to understand models’ decisions better. Combined with 3VL negatives tree generation we gain valuable insights into the underlying failure modes.

Note that removing less relevant tokens may enhance already existing biases. While Table VIII shows that this does

TABLE III
TOP-1 ACCURACY ON VSR [65] BENCHMARK, WITH OPENAI CLIP VIT-B/32, NEGCLIP [98], RB+LLM NEGS [1], AND 3VL.

Model	Accuracy
CLIP [48]	50.07
NegCLIP [98]	49.33
RB+LLM Negs [1]	50.21
Our 3VL	51.98

not amplify the bias, further reduction of the model bias is still required.

B. HilaCAM Anchor

We generate image-text pairs relevancy maps using HilaCAM [22]. In our case where a single image has more than one possible text, it is natural to calculate a different relevancy map for each image-text pair. Each of these relevancy maps can be used for *Token Removal*. We refer from now on to this natural way of calculating multiple relevancy maps per text as HilaCAM as well.

Another way to use HilaCAM in cases with a single image and few texts is to form a new single text from the given input texts and use this new text to generate a single relevancy map. One way to form such a new single text is to use only parts of texts that differ from one another.

For example, given the two texts, “*people playing with airborne frisbee*” and “*people playing with sitting frisbee*” we can generate the new text “*airborne frisbee or sitting frisbee*”. We refer to this new text as the “*Anchor*” text.

Having this *Anchor* text, we can generate a relevancy map from it and use it for *Token Removal*. *Anchor* with *Token Removal* is meant to focus both positive and negative texts on the same parts of the image. These parts of the image should contain the most important features for both positive and negative texts. Forcing a sort of cross-attention between the positive and negative texts.

TABLE IV
COCO IMAGE-TEXT RETRIEVAL WITH CLIP VIT-B/32, AND **3VL**

	I2T			T2I		
	R@1	R@5	R@10	R@1	R@5	R@10
CLIP [48]	32.54	57.7	68.08	28.66	53.04	64.44
3VL	33.72	62.08	73.12	36.54	63.32	74.48

TABLE V
FLICKR IMAGE-TEXT RETRIEVAL WITH CLIP VIT-B/32 AND **3VL**

	I2T			T2I		
	R@1	R@5	R@10	R@1	R@5	R@10
CLIP [48]	69.5	90.1	95	67	89.5	93.9
3VL	71	91.1	95.3	74	93.5	96.1

Anchor is especially useful when we have two texts that differ from each other only by one word. Such is the case with our caption tree generation method and the VL-CheckList [63] dataset. As we show in Section V, this leads to better interpretability and also to some performance gains as it makes the model more focused on the relevant parts of the image.

C. Differential Relevance (*DiRe*)

Another way to get a single relevancy map when we have two input texts, is to generate one relevancy map per text and then generate a new relevancy map by subtracting the negative relevancy map from the positive one. Although this method is not “fair” as we use the knowledge of which caption is positive and which is negative, we can still leverage this method combined with *Token Removal* for interpretability. The reason for that is that *DiRe* provides importance scores to the image tokens and it does not ‘directly intervene’ in the actual decision of the VLM. Therefore, if we find that the tokens of high relevancy according to *DiRe* correlate with better accuracy of the VLM, then we can get a better understanding of which tokens (that correspond to locations at the input image) affect the decision of the VLM and thus attain improved interpretability. In Figure 3 we show that indeed tokens of high relevancy according to *DiRe* correlate with better accuracy of the VLM (see details in Section V-D).

V. EXPERIMENTS

We evaluate our approach on popular Compositional Language Concepts benchmarks and on general downstream tasks. Then, we perform an interpretability assessment and examine CLIP failure modes and biases. We conclude this section with an ablation study.

A. 3VL Compositional Language Concepts Evaluation

We start by evaluating 3VL on the VL-Checklist. In the VL-Checklist [63] dataset we have a set of images and a pair of positive and negative captions for each image. The model is tested for image-text retrieval. The goal of this benchmark is to evaluate VLMs’ compositional understanding of objects, attributes and relations. Each negative caption is created by replacing one word in the positive sentence with respect to objects, relations or attributes.

We evaluate 3VL performance with and without *Token Removal*. Table I presents the results on the VL-Checklist

TABLE VI
CLIPSEG SEGMENTATION WITH CLIP VIT-B/32, AND **3VL**

	PhraseCut		COCO	
	IoU _{FG}	IoU _{BIN}	IoU _{FG}	IoU _{BIN}
CLIP [48]	52.4	71.7	54.8	73.2
3VL	53.4	72.1	57.2	74.7

TABLE VII
NUMBER OF FAILURES ON COCO TESTSET PER PART OF SPEECH TAG FOR VANILLA CLIP, NEGCLIP [98] AND **3VL**. **3VL** IMPROVES BY MORE THAN 50% ON VERBS(VERB) AND BY 46% ON ADPOSITIONS(ADP).

Model	NOUN	ADP	VERB	ADJ
CLIP	3104	2927	1612	913
NegCLIP	2743	1989	900	695
3VL	1976	1575	780	612

VG datasets [63], namely, VG Relation, Object and Attribute. Note that the VG datasets are the most challenging ones in the VL-Checklist benchmark. In the experiments, we compare our approach to openAI VIT-B/32 CLIP [48], NegCLIP [98], RB+LLM Negs [1]. The evaluation of the models’ performance involved measuring the Top-1 accuracy metric. Note the improvement in 3VL compared to the CLIP baseline and that our approach improves over the other techniques in most cases.

In addition, we evaluated the impact of using *Token Removal* (TR), where tokens were systematically removed from low to high importance according to *Anchor* (ANC) relevancy map as explained above. Note that *Token Removal* (TR) together with *Anchor* improves 3VL performance.

In Table II we add detailed results of VL-Checklist Object datasets, where we evaluate objects’ location invariance(e.g, center, middle, and margin) and size invariance (e.g., small, large, medium). A robust VLM should recognize objects’ existence, regardless of their location and size. Note the substantial performance improvement over all Object categories.

Table IX summarizes the results for the group categories of VL-Checklist. Notice that 3VL is significantly better than the other techniques on the relational and object categories. This may be attributed to the tree structure we introduce during training that helps in such type of queries. Yet, in attributes the improvement is better than NegCLIP but less than [1]. We conjecture that creating shallow rule-based hard negatives is more efficient for teaching attributes concepts like color and material while our tree structure is more beneficial for complex relational knowledge.

In addition, we report the results of 21 zero-shot tasks (ZS-Tasks). This includes Imagenet and the 20 tasks of ELEVATER [99]. This test checks the zero-shot image classification performance of our model and it shows that there is only little forgetting in our learning process. 3VL is better in this respect than NegCLIP but slightly worse than [1]. We also compare to CLIP and CLIP+LoRA finetuned on MS-COCO with contrastive loss (without tree augmented loss) as an ablation of the effects of finetuning on MSCOCO.

B. 3VL Visual Spatial Reasoning (VSR) Evaluation

The VSR [65] benchmark evaluates VLMs’ spatial reasoning using image-to-text retrieval. Each image contains a visible

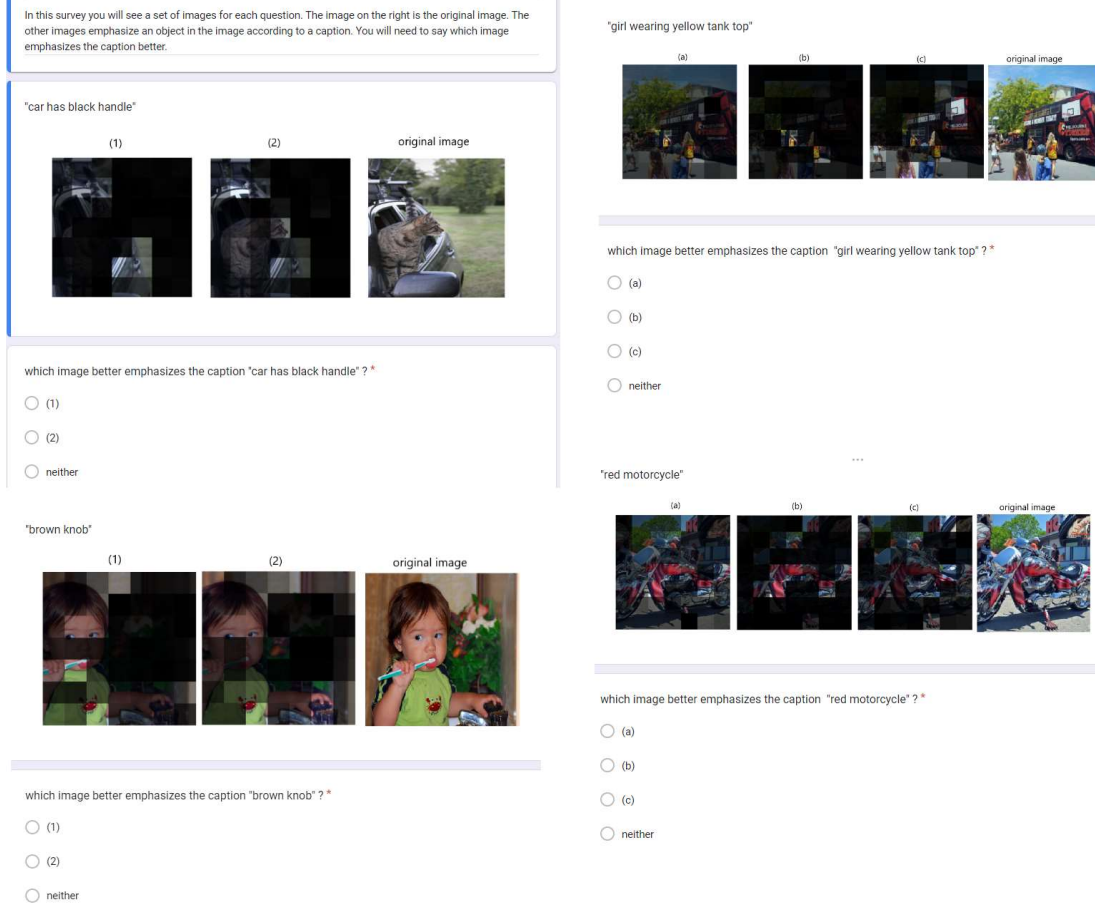


Fig. 4. A screen shot of some questions from the user study. The user-study instructions appear at the top left.

TABLE VIII
CLIP FAIL RATE ON SOME PAIRS OF POSITIVE-NEGATIVE WORDS ON
COCO TESTSET.

positive word	negative word	CLIP fail rate (%)	3VL fail rate (%)
small	large	50	35.8
large	small	25.26	22.1
on	off	35.74	20.5
off	on	78.26	50
young	old	23.57	4.5
old	young	50	28.2
down	up	55.26	35.03
up	down	44.08	19.2
white	black	22.17	13.87
black	white	27.35	23.36
man	woman	13.77	6.83
woman	man	17.6	14.18

spatial relation, and for each image we have a pair of captions with a description of this visible spatial relation and textual “True” and “False” labels concatenated at the end (e.g. “A is in front of B (False)”, “A is in front of B (True)”). The model needs to retrieve the caption with the correct label.

Table III presents the results of the VSR [65] dataset with openAI CLIP VIT-B/32, NegCLIP [98], RB+LLM Negs [1], and 3VL. Although this task is very hard for all models (probably somewhat because of the unusual caption + label prompt style) we can still see an advantage for 3VL.

C. 3VL Downstream Tasks Evaluation

We experimented on downstream tasks with the original CLIP model replaced by our 3VL and show the performance improvement of 3VL over CLIP.

Image-Text retrieval. In Tables IV and V we report results of image to text (I2T) and text to image (T2I) retrieval on COCO and FLICKR datasets.

Image Segmentation. Table VI reports segmentation results using CLIPSeg [100] with vanilla CLIP and with 3VL on COCO and PhraseCut [101] datasets.

D. Interpretability Quantitative Assessment

To assess the interpretability of our method, we follow the negative perturbation (*Token Removal*) test in [22]. First a relevancy map is extracted from the image-text pair. Then, we remove image tokens in order of increasing importance (from lowest to highest importance according to the relevancy map) and use the image with removed tokens as input to the image encoder and calculate the cosine similarity to both the positive text and negative text. As we have two texts, positive and negative, for HilaCAM [22] we calculate one relevancy map for the positive text and one for the negative text. Then, we remove tokens according to the relevancy map created by each of the texts and get two subsets of tokens which we

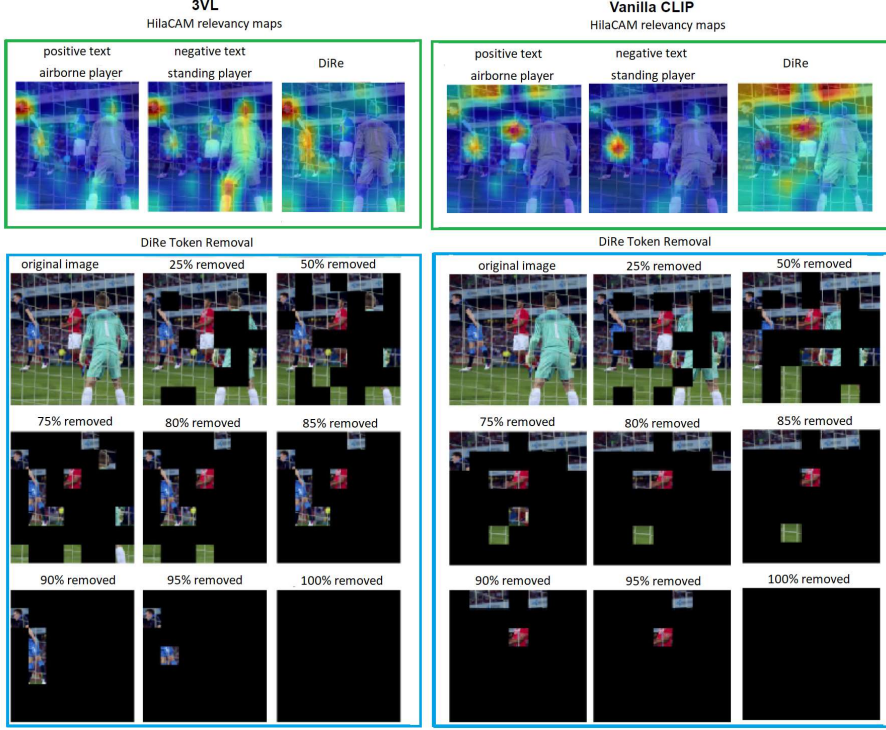


Fig. 5. A comparison of vanilla CLIP (right) and 3VL (left) interpretability for a randomly selected sample from the VL-Checklist VG attribute action dataset, where both models are mistaken. At the top we present the HilaCAM [22] relevancy map visualizations (red areas important, purple not important) for the positive text (“airborne player”) and negative text (“standing player”) and the *DiRe* relevancy map. On the second row from left to right we can see the *Token Removal* process. Starting from the original image we gradually remove the least significant tokens according to the *DiRe* relevancy map.

calculate cosine similarity for. For *Anchor* and *DiRe* we have only one relevancy map and we use it for *Token Removal*. The prediction in all cases is the text with the highest similarity score to the input image after *Token Removal*.

Figure 3 presents a negative perturbation test of 3VL and vanilla CLIP models together with HilaCAM [22], *Anchor* and *DiRe* relevancy maps. A more gradual decline in performance should point to a more explainable method as we remove less important tokens where importance is taken from that method’s relevancy map. We can see that *Anchor Token Removal* can improve performance which suggests that removing tokens using *Anchor* relevancy map focuses the model on the more important parts of the image. This strategy can also be used at inference time to improve the performance of VLMs.

DiRe creates a new relevancy map by subtracting the negative relevancy map from the positive relevancy map (both obtained from HilaCAM). Note that while *DiRe* cannot be used to improve accuracy at inference time (since it uses ground truth information about which input is positive and which is negative), it can be used to improve the interpretability of VLMs when analyzing a model and the ground truth is available. Figure 3 shows the advantage of *DiRe* for interpretability purposes as it emphasizes better the most informative tokens in the image.

1) *Interpretability User Study*: To further assess the interpretability of 3VL we conducted a user study. In the user study we have compared 3VL to vanilla CLIP using relevancy

maps generated from image-text pairs with *HilaCAM*, and we have compared relevancy maps generated by *HilaCAM* to relevancy maps generated by *Anchor* and *DiRe*. We have compared the different relevancy maps by letting users decide which relevancy map emphasizes a caption in an image better. We randomly sampled 25 images from the VL-Checklist VG dataset. For each image we presented the original image on the right and the relevancy maps (either *HilaCAM* relevancy maps for 3VL and vanilla CLIP, or the relevancy maps of *HilaCAM*, *Anchor* and *DiRe*) in random order. A total of 37 respondents participated in the study and were asked “which image better emphasizes the caption...” (a), (b), (c) or neither. We have found 3VL maps to be more explainable than vanilla CLIP. 51.67% of user choices were 3VL, 27.4% vanilla CLIP and 20.93% neither. Moreover, in 78.94% of the questions 3VL got the most votes. We have also found *DiRe* to be more explainable than *Anchor*, which is more explainable than *HilaCAM*. 57.6% of user choices were *DiRe*, 19.2% *Anchor*, 11.2% *HilaCAM* and 12% neither. Moreover, in 83.33% of the questions *DiRe* got the most votes and in 16.67% of the questions *Anchor* got the most votes. *HilaCAM* did not get the most votes in any of the questions. In Figure 4 we present some examples from the user study.

E. Interpretability Qualitative assessment

Figure 5 visualizes the strong interpretability of 3VL with HilaCAM and *DiRe*. We compare the visualizations of vanilla

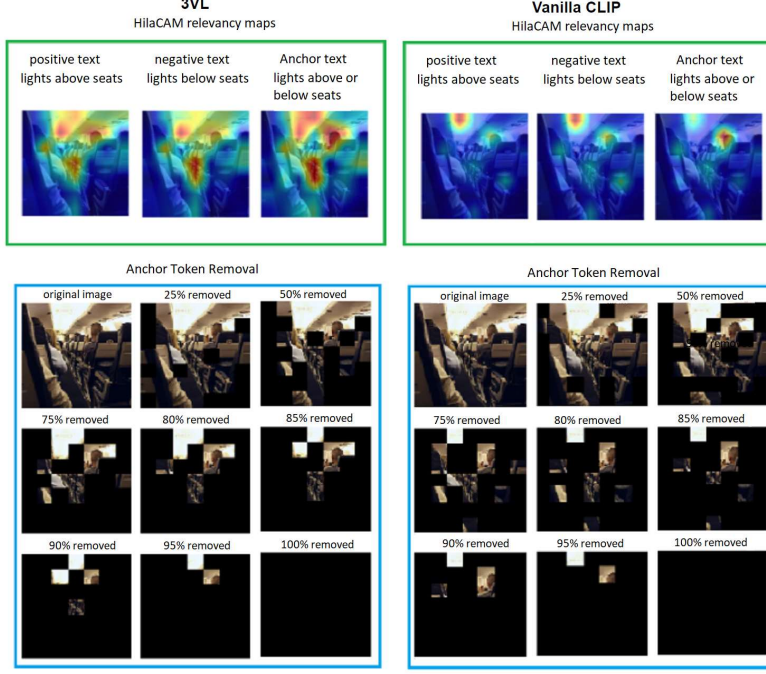


Fig. 6. A comparison between 3VL(left) and vanilla CLIP(right) visualizations with Anchor token removal. At the top: HilaCAM relevancy maps for positive text, negative text, and Anchor text ("light above seats", "light below seats", "light above or below seats"). At the bottom the input image with token removal (from 0% removal to 100%) according to Anchor relevancy map. 3VL attends to all lights in the photo, whereas Vanilla CLIP attends more to lights above seats. After Token removal, both attend to lights above seats.

CLIP and 3VL with HilaCAM [22] and 3VL on a random sample from the VL-Checklist dataset, where both CLIP and 3VL are mistaken. Note that from the HilaCAM visualizations it is hard to understand the source of the error. With 3VL the visualization of the positive text emphasizes an airborne player and the visualization of the negative text emphasizes both an airborne player and a standing player. With Vanilla CLIP the positive and negative visualizations emphasize different parts of airborne players. Yet both models mistakenly predict "standing player". When adding *DiRe* visualization we understand that the model should have focused more on the bottom part of the airborne player in addition to the upper part to understand that he is airborne. The *Token Removal* emphasizes this further. Figure 6 visualizes the strong interpretability of 3VL with HilaCAM and *Anchor*. 3VL attends to all lights in the photo, whereas Vanilla CLIP attends more to lights above seats. After Token removal, both attend to lights above seats.

F. Using 3VL for Understanding VLMs' Failures

Using our caption tree generation method we are able to find exact words and part of speech tags that the model fails to recognize. To offer extra insight regarding model's decisions, we expand the caption tree at the level in which the model failed, with extra words generated to be similar (co-hyponyms and synonyms) to the chosen negative word and to the positive word and check probability for all these words. We also add relative relevancy visualizations for these words at failure points. Figure 7 demonstrates how CLIP fails to understand multiple words phrases and considers each single word on its own. Figure 8 shows the relative relevancy maps of

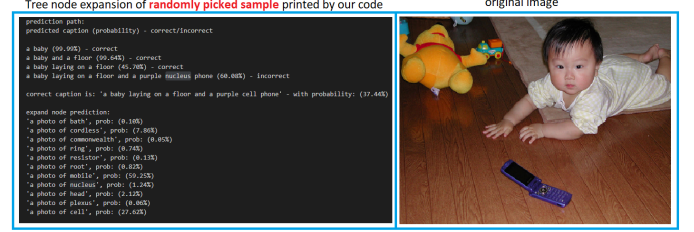


Fig. 7. Tree node expansion when the model confuses 'nucleus phone' and 'cell phone'. The model fails to understand the term 'cell phone' and interprets the word 'cell' as part of an organism, but when given the word 'mobile' instead of 'cell', the model identifies the mobile phone in the image and gives it a much higher probability than 'nucleus'.

the 4 most probable captions according to CLIP, highlighting different parts of the image for each(e.g. the wooden bench and the metal bench rail).

In Table VII we show statistics of failures per part-of-speech tag on MSCOCO test set with pretrained CLIP, ARO NegCLIP [98] and 3VL. Note the big improvement in some of CLIP's biggest weaknesses, verbs and adpositions understanding, with more than 50% improvement on verbs and 46% improvement on adpositions.

To gain a better understanding of the model's success and failures, we analyze the more frequent words failures and find some strong biases in vanilla CLIP. We show in Table VIII some CLIP biases and how it changes with 3VL.

G. Ablation Study

We conduct an ablation study to assess the impact of different factors on the effectiveness of our proposed tree-based

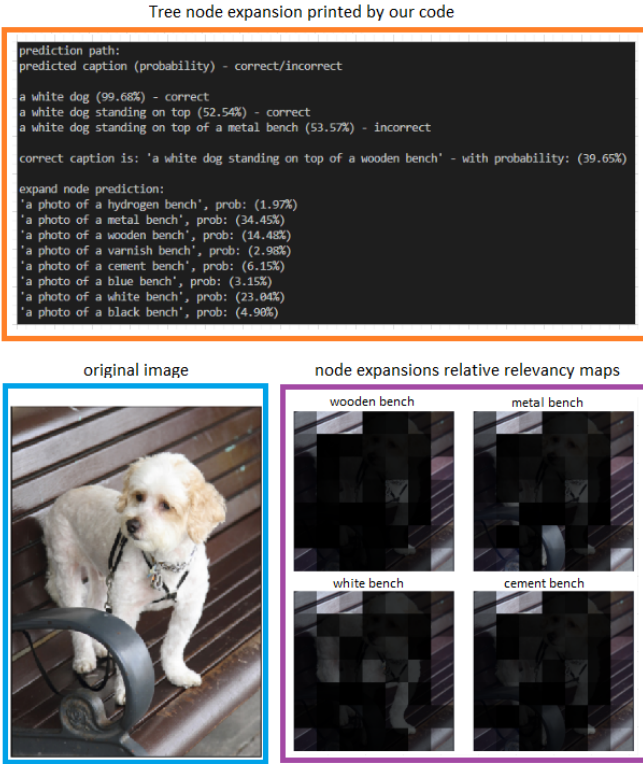


Fig. 8. A simple example of tree node expansion printed by our code (top left) in case of failure, the original image (bottom left), and relative relevancy maps (bottom right) of the top 4 most probable captions.

TABLE IX

TOP-1 ACCURACY ON VL-CHECKLIST(VLC) RELATION(REL) AVERAGE, ATTRIBUTE(ATTR) AVERAGE, OBJECT(OBJ) AVERAGE, AND AVERAGE ZERO-SHOT(ZS) ON ELEVATER 21 DATASETS. WE TEST ON OPENAI CLIP VIT-B/32, NEGCLIP [98], RB+LLM NEGS [1], AND 3VL. AS AN ABLATION WE ALSO COMPARE TO CLIP AND CLIP+LoRA THAT WERE TRAINED WITHOUT TREE-BASED LOSS.

Model	VLC-Attr	VLC-Rel	VLC-Obj	VLC-AVG	AVG 21 ZS-Tasks
CLIP [48]	69.25	58.35	79.01	68.87	56.37
CLIP contrastive	70.57	57.12	82.621	70.10	55.03
CLIP+LoRA contrastive	69.46	55.27	80.29	68.34	56.47
NegCLIP [98]	72.24	63.53	81.54	72.43	51.67
RB+LLM Negs [1]	78.49	74.20	84.34	79.01	54.66
Our 3VL CLIP	76.99	81.42	89.28	82.46	52.56

training technique. We examine the effects of different loss functions, different tree structures and negatives generation. We examine the regularization effects of limiting our caption tree to a maximum depth or limiting the number of maximum negatives generated in each tree.

Different loss functions ablation. In Table IX we show the impact of different loss functions on the performance of our model. Note that the addition of LoRA degrades a bit the performance on VL-checklist but reduces the forgetting effect (exhibited in the performance on ELEVATER [99]). Note that the addition of tree loss leads to a significant improvement over just using contrastive learning.

Caption tree variants ablation. In the tree training process of 3VL, we have explored many variants of caption tree structure, different negatives generation methods and their combinations. We provide below a detailed comparison between the different options using the example caption “several people standing in a green field together while flying kites”.

- **Tree structures.** We explored two main tree structures:

1) basic tree structure (“Basic”) where each noun phrase appears alone (without adding previous noun phrases and connecting text) in different tree levels and the full caption in the last tree level. (e.g. for the above example we will get a tree with 3 levels. “several people” in the first level, “a green field” in the second level, and “several people standing in a green field together while flying kites” in the third level).

2) incremental tree structure (“Incremental”) where each noun phrase is prepended once with previous tree level text only and once with previous tree level text plus the original text that connects to the current noun phrase (verbs and adpositions). (e.g. for the above example we will get a tree with 4 levels. “several people” in the first level, “several people and a green field” in the second level, “several people standing in a green field” in the third level, and “several people standing in a green field together while flying kites” in the fourth level).

- **Negatives generation.** We explored three main methods:
 - 1) Using WordNet (“WN”) replace nouns and verbs with co-hyponyms and replace adjectives and adpositions with antonyms or with random adjectives or adpositions.
 - 2) “LLM prompt” - we generate co-hyponyms, antonyms and random adjectives or adpositions with a prompt to FLAN-T5 (e.g., “find an opposite for the word: <>”).
 - 3) LLM mask completion (“LLM mask”) - generate a negative word by replacing a positive word with a mask token and passing it to T5 LLM [92] for mask completion. *Other methods include also replacing only nouns or verbs with mask completion.*

In Table X we show Top-1 accuracy results on VL-Checklist with four such tree variants. (i) “Basic WN” - “Basic” tree structure with WordNet negatives generation, (ii) “Incremental WN” - “Incremental” tree structure with WordNet negatives generation, (iii) “WN+LLM prompt+mask” - “Incremental” tree structure with “LLM prompt” for opposites generation, T5 mask completion for words with no opposite and WordNet replacement if T5 mask completion generates a word with similar meaning. (iv) “WN+LLM prompt (3VL)” - “Incremental” tree structure with “LLM prompt” for opposites generation and WordNet replacement if no opposite exists.

For each such variant, we report the highest result attained by hyperparameter sweep on the validation set of MSCOCO. We found that LLM mask completion oftentimes generated positive caption alternatives instead of negative captions and we did not use it in the final model. Best results were achieved using (iv) “WN+LLM prompt” and therefore, we used it in the final 3VL model.

H. Maximum tree depth ablation

In Table XI we report Top-1 accuracy on the VL-Checklist when constraining the 3VL tree to maximum depth. We note that we don’t limit here the number of generated negatives per caption, just the structure of the tree. So, for example, a tree of depth 1 will contain the same number of negatives as in the full caption tree, just in a single level. We can see that even though the number of negatives remains the same, the increase in tree depth contributes to improved performance.

TABLE X

TOP-1 ACCURACY ON VL-CHECKLIST FOR DIFFERENT CAPTION TREES. (I) “BASIC WN” - BASIC TREE STRUCTURE WITH WORDNET REPLACEMENT, (II) “INCREMENTAL WN” - INCREMENTAL TREE STRUCTURE WITH WORDNET REPLACEMENT, (III) “WN+LLM PROMPT+MASK” - INCREMENTAL TREE, FLAN-T5 PROMPT FOR OPPOSITES, T5 MASK COMPLETION IF OPPOSITE DOESN’T EXIST AND WORDNET REPLACEMENT IF MASK COMPLETION DID NOT GENERATE A WORD WITH A DIFFERENT MEANING. (IV) (“WN+LLM PROMPT (3VL)”) - INCREMENTAL TREE, FLAN-T5 PROMPT FOR OPPOSITES, AND WORDNET REPLACEMENT IF THE OPPOSITE DOES NOT EXIST.

Tree Method	Att color	Att material	Att size	Att action	Att state	Rel action	Rel spatial	Avg
Basic WN	70.54	75.79	69.72	75.95	70.46	81.81	73.94	74.03
Incremental WN	74.41	79.23	70.13	78.12	71.63	83.81	75.70	76.15
WN+LLM prompt+mask	72.31	77.53	69.98	76.69	69.39	83.43	76.87	75.17
WN+LLM prompt (3VL)	75.29	82.63	70.90	81.10	75.03	81.69	81.14	78.25

TABLE XI

TOP-1 ACCURACY ON VL-CHECKLIST WHEN CONSTRAINING 3VL TREE TO MAXIMUM DEPTH

Depth	Att color	Att material	Att size	Att action	Att state	Rel action	Rel spatial	Avg
1	72.70	78.42	69.28	78.81	70.99	78.54	74.10	74.69
2	72.99	79.51	69.24	79.81	72.90	79.04	74.49	75.43
3	73.27	79.43	68.68	80.97	72.79	80.99	78.55	76.38

TABLE XII

TOP-1 ACCURACY ON VL-CHECKLIST WHEN CONSTRAINING THE MAXIMUM TOTAL NUMBER OF GENERATED NEGATIVES PER TREE

Max negatives	Att color	Att material	Att size	Att action	Att state	Rel action	Rel spatial	Avg
1	72.47	75.22	66.35	73.31	72.69	69.80	53.70	69.08
2	73.24	77.49	69.39	75.05	73.96	75.15	65.67	72.85
4	74.16	78.18	70.28	77.59	73.54	79.86	74.18	75.39
8	74.29	79.72	70.54	76.06	75.56	80.31	79.08	76.50

I. Maximum negatives per tree ablation

In Table XII we report Top-1 accuracy on VL-Checklist when constraining the maximum total number of generated negatives per tree. We notice here the benefit in generating more negatives per caption.

J. Limitations

Note that although 3VL improves upon vanilla CLIP in all words, we sometimes see an increase in bias towards one word of a pair: Some pairs of words have a big gap between the fail rate when one of the words is the positive one and the other one is the negative word, compared to the fail rate with the same pair but with the positive and negative words switched. For example, as shown in Table VIII, when the word “small” is positive and the word “large” is negative CLIP has a 50% fail rate, but when the word “large” is the positive one and the word “small” is negative the fail rate is just above 25% which suggests a very strong bias of CLIP to the word “large” over “small”. With 3VL these fail rates are reduced to 35.8% and 22.1% and the gap is smaller. Yet, with the pairs “on”-“off” and “young”-“old” the bias is reduced a lot less with 3VL. Moreover, for the pairs “down”-“up”, “black”-“white”, and “man”-“woman” the gap even increases, although the model makes less mistakes overall. This is because the COCO train set contains an inherent large bias to one word from each of these pairs.

Having said that, we believe that the tree structure used with 3VL can be employed in order to decrease this gap. Given that we have the tree structure, we encourage a greater penalty on the tree leaves for text that appears less in the training data. We believe that our proposed tree augmentation method can be utilized to reduce biases in VLM training but we leave this direction to future work.

VI. CONCLUSION

In this work, we propose a novel approach to address the limitations of VLMs in Compositional Language Concepts

understanding and to enhance the interpretability of VLMs by leveraging the hierarchical structure of natural language. Our approach offers a richer exploration of the text space using several levels of incremental text augmentations from coarse to fine-grained, and in the process allows for better interpretation and analysis of model decisions. We complement our method with image heatmap relevancy maps of positive and negative texts and use this to identify further weaknesses of VLMs. We propose a new inference technique that effectively filters out the noise and irrelevant information from the input, allowing us to gain insights into the underlying failure modes of the model and achieve state-of-the-art performance on popular CLC benchmarks. We believe that our proposed tree augmentation method can be utilized to reduce biases in VLM training but we leave this direction to future work. Our work has important implications for the development of more interpretable and effective VLMs for natural language understanding and computer vision. Note that our proposed solution is generic. We have demonstrated it here with CLIP. Yet, a future work can easily incorporate it in other VLMs.

REFERENCES

- [1] S. Doveh, A. Arbelle, S. Harary, R. Panda, R. Herzig, E. Schwartz, D. Kim, R. Giryes, R. Feris, S. Ullman, and L. Karlinsky, “Teaching structured vision & language concepts to vision & language models,” in *CVPR*, 2023.
- [2] X. Hao, Y. Zhu, S. Appalaraju, A. Zhang, W. Zhang, B. Li, and M. Li, “Mixgen: A new multi-modal data augmentation,” in *WACV*, 2023.
- [3] P. Cascante-Bonilla, K. Shehada, J. S. Smith, S. Doveh, D. Kim, R. Panda, G. Varol, A. Oliva, V. Ordonez, R. Feris, and L. Karlinsky, “Going beyond nouns with vision & language models using synthetic data,” in *ICCV*, 2023.
- [4] A. Ray, K. Sikka, A. Divakaran, S. Lee, and G. Burachas, “Sunny and dark outside?! improving answer consistency in vqa through entailed question generation,” in *EMNLP*, 2019.
- [5] R. Tang, C. Ma, W. E. Zhang, Q. Wu, and X. Yang, “Semantic equivalent adversarial data augmentation for visual question answering,” in *European Conference on Computer Vision*, 2020, pp. 437–453.
- [6] K. Simonyan, A. Vedaldi, and A. Zisserman, “Deep inside convolutional networks: Visualising image classification models and saliency maps,” *arXiv preprint arXiv:1312.6034*, 2013.
- [7] R. R. Selvaraju, M. Cogswell, A. Das, R. Vedantam, D. Parikh, and D. Batra, “Grad-cam: Visual explanations from deep networks via gradient-based localization,” in *2017 IEEE International Conference on Computer Vision (ICCV)*, 2017, pp. 618–626.
- [8] M. T. Ribeiro, S. Singh, and C. Guestrin, ““why should i trust you?” explaining the predictions of any classifier,” in *ACM SIGKDD international conference on knowledge discovery and data mining*, 2016, pp. 1135–1144.
- [9] M. Sundararajan, A. Taly, and Q. Yan, “Axiomatic attribution for deep networks,” in *International conference on machine learning*, 2017, pp. 3319–3328.
- [10] S. M. Lundberg and S.-I. Lee, “A unified approach to interpreting model predictions,” *Advances in neural information processing systems*, vol. 30, 2017.
- [11] S. Kolek, D. A. Nguyen, R. Levie, J. Bruna, and G. Kutyniok, “Cartoon explanations of image classifiers,” in *ECCV*, 2022, pp. 443–458.

[12] S. Kolek, R. Windesheim, H. Andrade Loarca, G. Kutyniok, and R. Levie, “Explaining image classifiers with multiscale directional image representation,” in *IEEE Conference on Computer Vision and Pattern Recognition (CVPR)*, 2023.

[13] J. Adebayo, J. Gilmer, M. Muelly, I. Goodfellow, M. Hardt, and B. Kim, “Sanity checks for saliency maps,” in *Advances in neural information processing systems*, vol. 31, 2018.

[14] M. Yang and B. Kim, “Benchmarking attribution methods with relative feature importance,” 2019.

[15] P.-J. Kindermans, S. Hooker, J. Adebayo, M. Alber, K. T. Schütt, S. Dähne, D. Erhan, and B. Kim, “The (un)reliability of saliency methods,” 2017.

[16] H. Shah, P. Jain, and P. Netrapalli, “Do input gradients highlight discriminative features?” in *Advances in Neural Information Processing Systems*, vol. 34, 2021.

[17] D. Slack, S. Hilgard, E. Jia, S. Singh, and H. Lakkaraju, “Fooling lime and shap: Adversarial attacks on post hoc explanation methods,” in *AAAI/ACM Conference on AI, Ethics, and Society*, 2020, pp. 180–186.

[18] C. Rudin, “Stop explaining black box machine learning models for high stakes decisions and use interpretable models instead,” *Nature Machine Intelligence*, vol. 1, no. 5, pp. 206–215, 2019.

[19] P. W. Koh, T. Nguyen, Y. S. Tang, S. Mussmann, E. Pierson, B. Kim, and P. Liang, “Concept bottleneck models,” in *International Conference on Machine Learning*, 2020, pp. 5338–5348.

[20] A. Subramanya, V. Pillai, and H. Pirsiavash, “Fooling network interpretation in image classification,” in *IEEE/CVF International Conference on Computer Vision*, 2019, pp. 2020–2029.

[21] G. Schwalbe and B. Finzel, “A comprehensive taxonomy for explainable artificial intelligence: a systematic survey of surveys on methods and concepts,” *Data Mining and Knowledge Discovery*, 2023.

[22] H. Chefer, S. Gur, and L. Wolf, “Generic attention-model explainability for interpreting bi-modal and encoder-decoder transformers,” in *IEEE/CVF International Conference on Computer Vision (ICCV)*, October 2021, pp. 397–406.

[23] Y. Zhang, P. Tino, A. Leonardis, and K. Tang, “A survey on neural network interpretability,” *IEEE Transactions on Emerging Topics in Computational Intelligence*, vol. 5, no. 5, pp. 726–742, 2021.

[24] H. Chefer, S. Gur, and L. Wolf, “Transformer interpretability beyond attention visualization,” in *IEEE/CVF Conference on Computer Vision and Pattern Recognition (CVPR)*, June 2021, pp. 782–791.

[25] S. Bach, A. Binder, G. Montavon, F. Klauschen, K.-R. Müller, and W. Samek, “On pixel-wise explanations for non-linear classifier decisions by layer-wise relevance propagation,” *PloS one*, vol. 10, no. 7, p. e0130140, 2015.

[26] P.-J. Kindermans, S. Hooker, J. Adebayo, M. Alber, K. T. Schütt, S. Dähne, D. Erhan, and B. Kim, *The (Un)Reliability of Saliency Methods*, 2022, pp. 267–280.

[27] M. Bohle, M. Fritz, and B. Schiele, “Convolutional dynamic alignment networks for interpretable classifications,” in *IEEE/CVF Conference on Computer Vision and Pattern Recognition*, 2021, pp. 10 029–10 038.

[28] D. Alvarez Melis and T. Jaakkola, “Towards robust interpretability with self-explaining neural networks,” *Advances in neural information processing systems*, vol. 31, 2018.

[29] A. Chattopadhyay, S. Slocum, B. D. Haeffele, R. Vidal, and D. Geman, “Interpretable by design: Learning predictors by composing interpretable queries,” *IEEE Transactions on Pattern Analysis and Machine Intelligence*, vol. 45, no. 6, pp. 7430–7443, jun 2023.

[30] A. Chattopadhyay, K. H. R. Chan, B. D. Haeffele, D. Geman, and R. Vidal, “Variational information pursuit for interpretable predictions,” in *International Conference on Learning Representations*, 2023.

[31] C.-K. Yeh, B. Kim, S. Arik, C.-L. Li, T. Pfister, and P. Ravikumar, “On completeness-aware concept-based explanations in deep neural networks,” in *Advances in Neural Information Processing Systems*, vol. 33, 2020, pp. 20 554–20 565.

[32] J. Donnelly, A. J. Barnett, and C. Chen, “Deformable protopnet: An interpretable image classifier using deformable prototypes,” in *IEEE/CVF Conference on Computer Vision and Pattern Recognition*, 2022, pp. 10 265–10 275.

[33] M. Nauta, R. van Bree, and C. Seifert, “Neural prototype trees for interpretable fine-grained image recognition,” in *IEEE/CVF Conference on Computer Vision and Pattern Recognition*, 2021, pp. 14 933–14 943.

[34] A. Sarkar, D. Vijaykeerthy, A. Sarkar, and V. N. Balasubramanian, “A framework for learning ante-hoc explainable models via concepts,” in *IEEE/CVF Conference on Computer Vision and Pattern Recognition*, 2022, pp. 10 286–10 295.

[35] D. Lindner, J. Kramár, M. Rahtz, T. McGrath, and V. Mikulik, “Tracr: Compiled transformers as a laboratory for interpretability,” *arXiv preprint arXiv:2301.05062*, 2023.

[36] C. Mao, R. Teotia, A. Sundar, S. Menon, J. Yang, X. Wang, and C. Vondrick, “Doubly right object recognition: A why prompt for visual rationales,” in *CVPR*, 2023.

[37] L. Karlinsky, J. Shtok, A. Alfassy, M. Lichtenstein, S. Harary, E. Schwartz, S. Doveh, P. Sattigeri, R. Feris, A. Bronstein *et al.*, “Starinet: towards weakly supervised few-shot object detection,” in *AAAI Conference on Artificial Intelligence*, vol. 35, no. 2, 2021, pp. 1743–1753.

[38] H. Li, J. Song, M. Xue, H. Zhang, J. Ye, L. Cheng, and M. Song, “A survey of neural trees,” *arXiv preprint arXiv:2209.03415*, 2022.

[39] K. S. Tai, R. Socher, and C. D. Manning, “Improved semantic representations from tree-structured long short-term memory networks,” in *ACL*, 2015.

[40] D. Liu, H. Zhang, F. Wu, and Z.-J. Zha, “Learning to assemble neural module tree networks for visual grounding,” in *IEEE/CVF International Conference on Computer Vision*, 2019, pp. 4673–4682.

[41] P. Kotschieder, M. Fiterau, A. Criminisi, and S. R. Bulo, “Deep neural decision forests,” in *IEEE International Conference on Computer Vision (ICCV)*, December 2015.

[42] R. Tanno, K. Arulkumaran, D. Alexander, A. Criminisi, and A. Nori, “Adaptive neural trees,” in *International Conference on Machine Learning*, ser. Proceedings of Machine Learning Research, vol. 97, 09–15 Jun 2019, pp. 6166–6175.

[43] B. Wan, W. Han, Z. Zheng, and T. Tuytelaars, “Unsupervised vision-language grammar induction with shared structure modeling,” in *International Conference on Learning Representations*, 2022.

[44] M. Wu, S. Parbhoo, M. C. Hughes, V. Roth, and F. Doshi-Velez, “Optimizing for interpretability in deep neural networks with tree regularization,” *Journal of Artificial Intelligence Research*, vol. 72, pp. 1–37, 2021.

[45] Y. Ding, L. Wang, H. Zhang, J. Yi, D. Fan, and B. Gong, “Defending against adversarial attacks using random forest,” in *IEEE/CVF Conference on Computer Vision and Pattern Recognition Workshops (CVPRW)*, 2019, pp. 105–114.

[46] G. Cohen and R. Giryes, “Simple post-training robustness using test time augmentations and random forest,” 2021.

[47] A. Wan, L. Dunlap, D. Ho, J. Yin, S. Lee, S. Petryk, S. A. Bargal, and J. E. Gonzalez, “{NBDT}: Neural-backed decision tree,” in *International Conference on Learning Representations*, 2021.

[48] A. Radford, J. W. Kim, C. Hallacy, A. Ramesh, G. Goh, S. Agarwal, G. Sastry, A. Askell, P. Mishkin, J. Clark *et al.*, “Learning transferable visual models from natural language supervision,” in *International Conference on Machine Learning*, 2021, pp. 8748–8763.

[49] C. Jia, Y. Yang, Y. Xia, Y.-T. Chen, Z. Parekh, H. Pham, Q. Le, Y.-H. Sung, Z. Li, and T. Duerig, “Scaling up visual and vision-language representation learning with noisy text supervision,” in *International Conference on Machine Learning*, 2021, pp. 4904–4916.

[50] H. Tan and M. Bansal, “Lxmert: Learning cross-modality encoder representations from transformers,” in *EMNLP*, 2019.

[51] Y.-C. Chen, L. Li, L. Yu, A. El Kholy, F. Ahmed, Z. Gan, Y. Cheng, and J. Liu, “Uniter: Universal image-text representation learning,” in *European conference on computer vision*, 2020, pp. 104–120.

[52] X. Li, X. Yin, C. Li, P. Zhang, X. Hu, L. Zhang, L. Wang, H. Hu, L. Dong, F. Wei *et al.*, “Oscar: Object-semantics aligned pre-training for vision-language tasks,” in *European Conference on Computer Vision*, 2020, pp. 121–137.

[53] O. Russakovsky, J. Deng, H. Su, J. Krause, S. Satheesh, S. Ma, Z. Huang, A. Karpathy, A. Khosla, M. Bernstein *et al.*, “Imagenet large scale visual recognition challenge,” *International journal of computer vision*, vol. 115, no. 3, pp. 211–252, 2015.

[54] T.-Y. Lin, M. Maire, S. Belongie, J. Hays, P. Perona, D. Ramanan, P. Dollár, and C. L. Zitnick, “Microsoft coco: Common objects in context,” in *European conference on computer vision*, 2014, pp. 740–755.

[55] L. Yao, R. Huang, L. Hou, G. Lu, M. Niu, H. Xu, X. Liang, Z. Li, X. Jiang, and C. Xu, “FILIP: Fine-grained interactive language-image pre-training,” in *International Conference on Learning Representations*, 2022.

[56] S. Goel, H. Bansal, S. Bhatia, R. A. Rossi, V. Vinay, and A. Grover, “Cyclip: Cyclic contrastive language-image pretraining,” *arXiv preprint arXiv:2205.14459*, 2022.

[57] Y. Li, F. Liang, L. Zhao, Y. Cui, W. Ouyang, J. Shao, F. Yu, and J. Yan, “Supervision exists everywhere: A data efficient contrastive language-image pre-training paradigm,” *arXiv preprint arXiv:2110.05208*, 2021.

[58] Y. Gao, J. Liu, Z. Xu, J. Zhang, K. Li, and C. Shen, “Pyramidclip: Hierarchical feature alignment for vision-language model pretraining,” *arXiv preprint arXiv:2204.14095*, 2022.

[59] W. Kim, B. Son, and I. Kim, “Vilt: Vision-and-language transformer without convolution or region supervision,” in *International Conference on Machine Learning*, 2021, pp. 5583–5594.

[60] J. Yang, J. Duan, S. Tran, Y. Xu, S. Chanda, L. Chen, B. Zeng, T. Chilimbi, and J. Huang, “Vision-language pre-training with triple contrastive learning,” in *IEEE/CVF Conference on Computer Vision and Pattern Recognition*, 2022, pp. 15 671–15 680.

[61] M. Shukor, G. Couairon, and M. Cord, “Efficient vision-language pretraining with visual concepts and hierarchical alignment,” in *33rd British Machine Vision Conference (BMVC)*, 2022.

[62] J. Li, D. Li, C. Xiong, and S. Hoi, “Blip: Bootstrapping language-image pre-training for unified vision-language understanding and generation,” in *ICML*, 2022.

[63] T. Zhao, T. Zhang, M. Zhu, H. Shen, K. Lee, X. Lu, and J. Yin, “Vi-checklist: Evaluating pre-trained vision-language models with objects, attributes and relations,” *arXiv preprint arXiv:2207.00221*, 2022.

[64] T. Thrush, R. Jiang, M. Bartolo, A. Singh, A. Williams, D. Kiela, and C. Ross, “Winoground: Probing vision and language models for visiolinguistic compositionality,” in *IEEE/CVF Conference on Computer Vision and Pattern Recognition*, 2022, pp. 5238–5248.

[65] F. Liu, G. E. T. Emerson, and N. Collier, “Visual spatial reasoning,” *Transactions of the Association for Computational Linguistics*, 2023.

[66] A. Ray, F. Radenovic, A. Dubey, B. A. Plummer, R. Krishna, and K. Saenko, “Cola: How to adapt vision-language models to compose objects localized with attributes?” 2023.

[67] N. Dziri, X. Lu, M. Sclar, X. L. Li, L. Jiang, B. Y. Lin, P. West, C. Bhagavatula, R. L. Bras, J. D. Hwang, S. Sanyal, S. Welleck, X. Ren, A. Ettinger, Z. Harchaoui, and Y. Choi, “Faith and fate: Limits of transformers on compositionality,” in *NeurIPS*, 2023.

[68] Y.-C. Chen, L. Li, L. Yu, A. E. Kholy, F. Ahmed, Z. Gan, Y. Cheng, and J. Liu, “Uniter: Universal image-text representation learning,” in *ECCV*, 2020.

[69] L. H. Li, M. Yatskar, D. Yin, C.-J. Hsieh, and K.-W. Chang, “Visu-albert: A simple and performant baseline for vision and language,” *ArXiv*, vol. abs/1908.03557, 2019.

[70] H. H. Tan and M. Bansal, “Lxmert: Learning cross-modality encoder representations from transformers,” in *EMNLP*, 2019.

[71] D. Xu, Y. Zhu, C. B. Choy, and L. Fei-Fei, “Scene Graph Generation by Iterative Message Passing,” in *CVPR*, 2017, pp. 3097–3106.

[72] R. Herzig, M. Raboh, G. Chechik, J. Berant, and A. Globerson, “Mapping images to scene graphs with permutation-invariant structured prediction,” in *Advances in Neural Information Processing Systems*, 2018.

[73] R. Krishna, I. Chami, M. S. Bernstein, and L. Fei-Fei, “Referring relationships,” *ECCV*, 2018.

[74] A. Jerbi, R. Herzig, J. Berant, G. Chechik, and A. Globerson, “Learning object detection from captions via textual scene attributes,” *ArXiv*, vol. abs/2009.14558, 2020.

[75] M. Raboh, R. Herzig, G. Chechik, J. Berant, and A. Globerson, “Differentiable scene graphs,” in *WACV*, 2020.

[76] F. Baradel, N. Neverova, C. Wolf, J. Mille, and G. Mori, “Object level visual reasoning in videos,” in *ECCV*, 2018, pp. 105–121.

[77] P. W. Battaglia, J. B. Hamrick, V. Bapst, A. Sanchez-Gonzalez, V. Zambaldi, M. Malinowski, A. Tacchetti, D. Raposo, A. Santoro, R. Faulkner *et al.*, “Relational inductive biases, deep learning, and graph networks,” *arXiv preprint arXiv:1806.01261*, 2018.

[78] C. Gao, J. Xu, Y. Zou, and J.-B. Huang, “Drg: Dual relation graph for human-object interaction detection,” *ArXiv*, vol. abs/2008.11714, 2020.

[79] K. Kato, Y. Li, and A. Gupta, “Compositional learning for human object interaction,” in *ECCV*, 2018.

[80] B. Xu, Y. Wong, J. Li, Q. Zhao, and M. Kankanhalli, “Learning to detect human-object interactions with knowledge,” *2019 IEEE/CVF Conference on Computer Vision and Pattern Recognition (CVPR)*, pp. 2019–2028, 2019.

[81] E. B. Avraham, R. Herzig, K. Mangalam, A. Bar, A. Rohrbach, L. Karlinsky, T. Darrell, and A. Globerson, “Bringing image scene structure to video via frame-clip consistency of object tokens,” in *Thirty-Sixth Conference on Neural Information Processing Systems*, 2022.

[82] A. Arnab, C. Sun, and C. Schmid, “Unified graph structured models for video understanding,” in *ICCV*, 2021.

[83] J. Materzynska, T. Xiao, R. Herzig, H. Xu, X. Wang, and T. Darrell, “Something-else: Compositional action recognition with spatial-temporal interaction networks,” in *IEEE Conference on Computer Vision and Pattern Recognition*, 2020.

[84] R. Herzig, E. Ben-Avraham, K. Mangalam, A. Bar, G. Chechik, A. Rohrbach, T. Darrell, and A. Globerson, “Object-region video transformers,” in *Conference on Computer Vision and Pattern Recognition (CVPR)*, 2022.

[85] R. Herzig, E. Levi, H. Xu, H. Gao, E. Brosh, X. Wang, A. Globerson, and T. Darrell, “Spatio-temporal action graph networks,” in *IEEE International Conference on Computer Vision Workshops*, 2019.

[86] J. Ji, R. Krishna, L. Fei-Fei, and J. C. Niebles, “Action genome: Actions as composition of spatio-temporal scene graphs,” *arXiv preprint arXiv:1912.06992*, 2019.

[87] X. Wang and A. Gupta, “Videos as space-time region graphs,” in *ECCV*, 2018.

[88] A. Bar, R. Herzig, X. Wang, A. Rohrbach, G. Chechik, T. Darrell, and A. Globerson, “Compositional video synthesis with action graphs,” in *ICML*, 2021.

[89] R. Herzig, A. Bar, H. Xu, G. Chechik, T. Darrell, and A. Globerson, “Learning canonical representations for scene graph to image generation,” in *European Conference on Computer Vision*, 2020.

[90] J. Johnson, A. Gupta, and L. Fei-Fei, “Image generation from scene graphs,” in *IEEE conference on computer vision and pattern recognition*, 2018, pp. 1219–1228.

[91] M. Honnibal and I. Montani, “spaCy 2: Natural language understanding with Bloom embeddings, convolutional neural networks and incremental parsing,” 2017, to appear.

[92] H. W. Chung, L. Hou, S. Longpre, B. Zoph, Y. Tay, W. Fedus, Y. Li, X. Wang, M. Dehghani, S. Brahma, A. Webson, S. S. Gu, Z. Dai, M. Suzgun, X. Chen, A. Chowdhery, A. Castro-Ros, M. Pellat, K. Robinson, D. Valter, S. Narang, G. Mishra, A. Yu, V. Zhao, Y. Huang, A. Dai, H. Yu, S. Petrov, E. H. Chi, J. Dean, J. Devlin, A. Roberts, D. Zhou, Q. V. Le, and J. Wei, “Scaling instruction-finetuned language models,” 2022.

[93] S. Bird, E. Klein, and E. Loper, *Natural language processing with Python: analyzing text with the natural language toolkit*. ” O’Reilly Media, Inc., 2009.

[94] G. A. Miller, “Wordnet: A lexical database for english,” *Communications of the ACM*, vol. 38, no. 11, pp. 39–41, 1995.

[95] C. Raffel, N. Shazeer, A. Roberts, K. Lee, S. Narang, M. Matena, Y. Zhou, W. Li, and P. J. Liu, “Exploring the limits of transfer learning with a unified text-to-text transformer,” *The Journal of Machine Learning Research*, vol. 21, no. 1, pp. 5485–5551, 2020.

[96] E. J. Hu, yelong shen, P. Wallis, Z. Allen-Zhu, Y. Li, S. Wang, L. Wang, and W. Chen, “LoRA: Low-rank adaptation of large language models,” in *International Conference on Learning Representations*, 2022.

[97] A. Dosovitskiy, L. Beyer, A. Kolesnikov, D. Weissenborn, X. Zhai, T. Unterthiner, M. Dehghani, M. Minderer, G. Heigold, S. Gelly *et al.*, “An image is worth 16x16 words: Transformers for image recognition at scale,” in *International Conference on Learning Representations*.

[98] M. Yuksekgonul, F. Bianchi, P. Kalluri, D. Jurafsky, and J. Zou, “When and why vision-language models behave like bags-of-words, and what to do about it?” in *International Conference on Learning Representations*, 2023.

[99] C. Li, H. Liu, L. H. Li, P. Zhang, J. Aneja, J. Yang, P. Jin, Y. J. Lee, H. Hu, Z. Liu, and J. Gao, “Elevater: A benchmark and toolkit for evaluating language-augmented visual models,” *Neural Information Processing Systems*, 2022.

[100] T. Lüddecke and A. Ecker, “Image segmentation using text and image prompts,” in *IEEE/CVF Conference on Computer Vision and Pattern Recognition (CVPR)*, 2022, pp. 7086–7096.

[101] C. Wu, Z. Lin, S. Cohen, T. Bui, and S. Maji, “Phrasecut: Language-based image segmentation in the wild,” 2020.